

12-11-2012

Targeted Disruption of Adamts16 Gene in a Rat Genetic Model of Hypertension

Kathirvel Gopalakrishnan
University of Toledo

Sivarajan Kumarasamy
University of Toledo


Shakila Abdul-Majeed
University of Toledo

Andrea L. Kalinoski
University of Toledo

Eric E. Morgan
University of Toledo

See next page for additional authors

Follow this and additional works at: http://digitalcommons.chapman.edu/pharmacy_articles

 Part of the [Animal Structures Commons](#), [Cardiology Commons](#), [Cardiovascular System Commons](#), and the [Circulatory and Respiratory Physiology Commons](#)

Recommended Citation

Gopalakrishnan K, Kumarasamy S, Abdul-Majeed S, Kalinoski AL, Morgan EE, Gohara AF, Nauli SM, Filipiak WE, Saunders TL, Joe B. Targeted disruption of Adamts16 gene in a rat genetic model of hypertension. *Proc Natl Acad Sci USA*. 2012 Dec 11;109(50):20555-9.
DOI: 10.1073/pnas.1211290109

This Article is brought to you for free and open access by the School of Pharmacy at Chapman University Digital Commons. It has been accepted for inclusion in Pharmacy Faculty Articles and Research by an authorized administrator of Chapman University Digital Commons. For more information, please contact laughtin@chapman.edu.

Targeted Disruption of Adamts16 Gene in a Rat Genetic Model of Hypertension

Comments

This article was originally published in *Proceedings of the National Academy of Sciences*, volume 109, issue 50, in December 2012. DOI: [10.1073/pnas.1211290109](https://doi.org/10.1073/pnas.1211290109)

Copyright

National Academy of Sciences

Authors

Kathirvel Gopalakrishnan, Sivarajan Kumarasamy, Shakila Abdul-Majeed, Andrea L. Kalinoski, Eric E. Morgan, Amira F. Gohara, Surya M. Nauli, Wanda E. Filipiak, Thomas L. Saunders, and Bina Joe

Targeted disruption of *Adamts16* gene in a rat genetic model of hypertension

Kathirvel Gopalakrishnan^{a,b}, Sivarajan Kumarasamy^{a,b}, Shakila Abdul-Majeed^{a,b}, Andrea L. Kalinoski^{a,c}, Eric E. Morgan^{b,d}, Amira F. Gohara^e, Surya M. Nauli^{a,f}, Wanda E. Filipiak^g, Thomas L. Saunders^g, and Bina Joe^{a,b,1}

^aCenter for Hypertension and Personalized Medicine, ^bDepartment of Physiology and Pharmacology, ^cDepartment of Surgery, ^dCenter for Diabetes and Endocrine Research, ^eDepartment of Pathology, University of Toledo College of Medicine and Life Sciences, Toledo, OH 43614; ^fDepartment of Pharmacology, University of Toledo College of Pharmacy, Toledo, OH 43614; and ^gTransgenic Animal Model Core, University of Michigan Medical School, Ann Arbor, MI 48109

Edited by Iva Greenwald, Columbia University, New York, NY, and approved October 26, 2012 (received for review July 5, 2012)

A disintegrin-like metalloproteinase with thrombospondin motifs–16 (*Adamts16*) is an important candidate gene for hypertension. The goal of the present study was to further assess the candidacy of *Adamts16* by targeted disruption of this gene in a rat genetic model of hypertension. A rat model was generated by manipulating the genome of the Dahl Salt-sensitive (S) rat using zinc-finger nucleases, wherein the mutant rat had a 17 bp deletion in the first exon of *Adamts16*, introducing a stop codon in the transcript. Systolic blood pressure (BP) of the homozygous *Adamts16*^{mutant} rats was lower by 36 mmHg compared with the BP of the S rats. The *Adamts16*^{mutant} rats exhibited significantly lower aortic pulse wave velocity and vascular media thickness compared with S rats. Scanning electron and fluorescence microscopic studies indicated that the mechanosensory cilia of vascular endothelial cells from the *Adamts16*^{mutant} rats were longer than that of the S rats. Furthermore, *Adamts16*^{mutant} rats showed splitting and thickening of glomerular capillaries and had a longer survival rate, compared with the S rats. Taken together, these physiological observations functionally link *Adamts16* to BP regulation and suggest the vasculature as the potential site of action of *Adamts16* to lower BP.

congenic | mapping | ZFN mutant | quantitative trait locus | GWAS

Despite strong evidence that susceptibility or resistance to the development of hypertension is heritable, the identification of genetic variants that cause blood pressure (BP) to rise into a hypertensive state has remained difficult (1, 2). Classic genetic mapping and association studies in both humans and in rats point to several genetic elements as potential candidates causing hypertension (3, 4). Most of the prioritized candidate genes for hypertension await functional assessments.

Linkage analysis in the Quebec Family Study identified a quantitative trait locus (QTL) for systolic BP on human chromosome 5p15 (5). The corresponding comparative segment of human chromosome 5p15 on rat chromosome 1 is also linked to a BP QTL in rats (6). Improved resolutions of this locus in rats were obtained through iterative substitution mapping using strains differentially susceptible to the development of hypertension (6–10). A disintegrin-like metalloproteinase with thrombospondin motifs–16 (*Adamts16*), which was the only known gene with exonic variants within the highly resolved congenic interval, was prioritized as a candidate BP quantitative trait gene (QTG) (8). More importantly, following the congenic mapping study in rats, human allelic variants of *Adamts16* were confirmed as being associated with BP in two independent cohorts, one of which was the Quebec Family Study (8). Taken together, all these studies point to *Adamts16* as a prominent candidate locus linked to BP control across two species. However, due to the limitations of recombination frequencies, both the linkage and substitution mapping studies in rats cannot validate *Adamts16* as the BP QTG because of the presence of other candidate variants within the linked or introgressed flanking genomic segments, respectively. Until recently, targeted gene functional studies were impossible in

the rat due to technical limitations of site-targeted gene editing strategies. In 2009, a technique of zinc-finger nuclease (ZFN)-mediated targeted gene disruption was successfully described in the rat (11). The goal of the current study was to apply this targeted gene-disruption strategy to assess the functional link between *Adamts16* and BP.

In this study we describe the creation of a rat *Adamts16*^{mutant} model using the ZFN method. The characterization of this model demonstrates the functional link between *Adamts16* and BP. Further, the vasculature was identified as one of the potential target tissues affected by the disruption of the *Adamts16* gene. In summary, this study applied a gene-targeting approach for direct physiological assessment of a candidate gene previously mapped to a high resolution using linkage and substitution mapping in rats.

Results

Targeted Mutation of *Adamts16* Decreased BP. The *Adamts16*^{mutant} rats had a shorter (290 bp) PCR-amplified genomic DNA fragment compared with the Dahl Salt-sensitive (S) (307 bp) genomic fragment (Fig. 1A). The 17 bp deletion within exon 1 of *Adamts16* of these PCR fragments was confirmed by sequencing (Fig. 1B). cDNA isolated from the *Adamts16*^{mutant} rats also reflected this 17 bp deletion (Fig. 1B). Both the homozygous and heterozygous *Adamts16*^{mutant} rats appeared healthy and gained weight similar to the S rats. BP of the homozygous *Adamts16*^{mutant} rats, as measured by the tail-cuff method, were significantly lower by 36 mmHg compared with the BP of the S rats (184 ± 1.16 versus 220 ± 3.64 mmHg, $P < 0.001$) (Fig. 2A). Similarly, the BP of the heterozygous *Adamts16*^{mutant} rats was also lower than the BP of the S rats by 14 mmHg (198 ± 4.94 versus 220 ± 3.64 mmHg, $P < 0.01$) (Fig. 2A). To further confirm these observations, rats were surgically implanted with radiotransmitters and BP was continuously recorded by telemetry. During all of the 5 d of observation, both systolic and diastolic pressure of both homozygous and heterozygous *Adamts16*^{mutant} rats were consistently lower than that of the S rats (Fig. 2B and C).

Decreased Pulse Wave Velocity and Media Thickness in *Adamts16*^{mutant} Rats. In accordance with the changes in BP, the heart weight–body weight ratios of the *Adamts16*^{mutant} rats were lower than that of the S rats (Fig. 3A). When the animals were examined by echocardiography, the left ventricular relative wall thickness (RWT) and aortic pulse wave velocity (PWV) of both the homozygous and heterozygous *Adamts16*^{mutant} rats were lower

Author contributions: B.J. designed research; K.G., S.K., S.A.-M., A.L.K., E.E.M., A.F.G., S.M.N., W.E.F., T.L.S., and B.J. performed research; K.G., S.K., S.A.-M., A.L.K., E.E.M., A.F.G., and S.M.N. analyzed data; and K.G. and B.J. wrote the paper.

The authors declare no conflict of interest.

This article is a PNAS Direct Submission.

Freely available online through the PNAS open access option.

¹To whom correspondence should be addressed. E-mail: bina.joe@utoledo.edu.

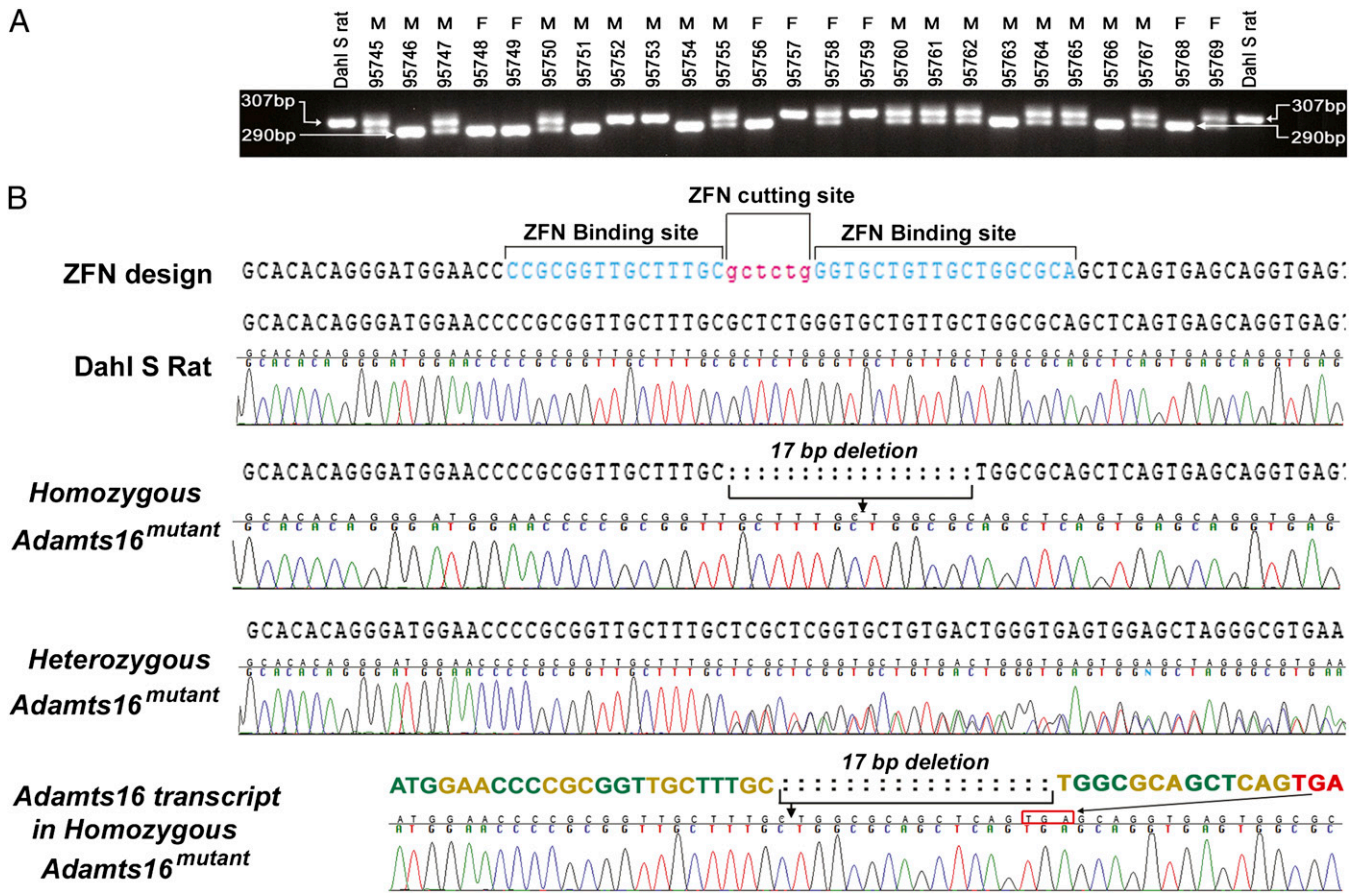


Fig. 1. Screening animals for ZFN-targeted mutation at the *Adams16* locus. (A) Representative agarose gel image of PCR-amplified genomic DNA from an intercross of heterozygous *Adams16*^{mutant} carriers. The normal allele of the Dahl S rat is 307 bp. Rats with alternate allele size of 290 bp are representative mutants. M, males; F, females; 95745–95769, rat tag numbers. (B) Representative sequencing results from the 307 bp and 290 bp bands shown in panel A confirmed the 17 bp deletion in the genomic DNA. The same 17 bp deletion was confirmed by amplification and sequencing of cDNA from the homozygous mutants. TGA in red depicts the stop codon in exon 1.

than that of the S rats (Fig. 3 B and C). This was interesting because PWV is a measure of arterial stiffness (12). Elevated PWV and thereby increased arterial stiffness is an independent marker of cardiovascular risk in human hypertension (13). Therefore, we examined the structure of the abdominal aorta more closely by second harmonic generation microscopy. As seen

in Fig. 4A, the media area of aortae from the homozygous *Adams16*^{mutant} rats were lower than that of the control S rat.

Endothelial Cells from the *Adams16*^{mutant} Rats Have Elongated Cilia.

To further evaluate phenotypic differences in the vasculature, we examined cilia within the endothelial cells of arteries. Cilia are

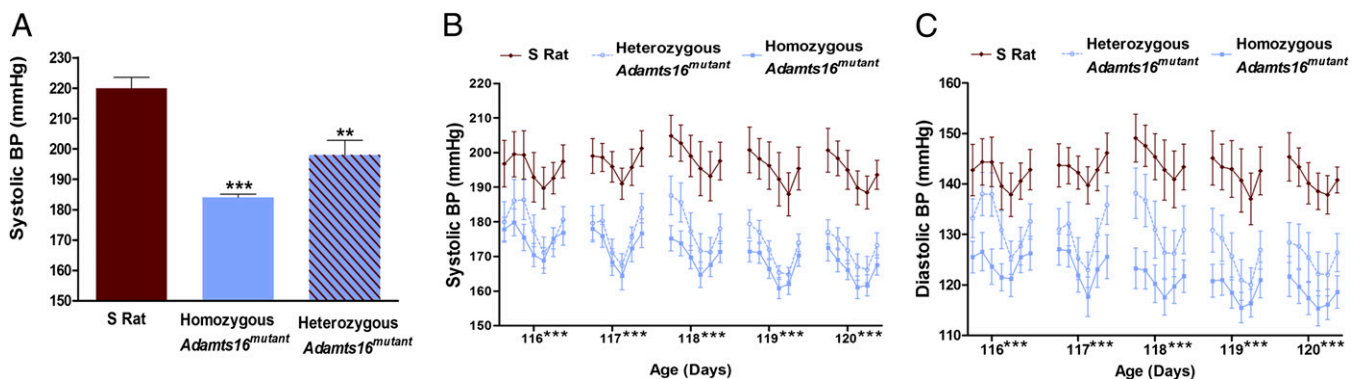


Fig. 2. BP measurements of homozygous *Adams16*^{mutant} ($n = 6$), heterozygous *Adams16*^{mutant} ($n = 5$), and S ($n = 7$) rats. Levels of statistical significance for all data were analyzed by ANOVA followed by Tukey's test. (A) Mean systolic BP effect \pm SEM by the tail-cuff method. (B and C) BP measures of the same animals monitored after surgical implantation of radiotelemetry transmitters. Data plotted are the recordings obtained once every 5 min continuously for 24 h and averaged for 4 h intervals; ** $P < 0.01$, *** $P < 0.001$.

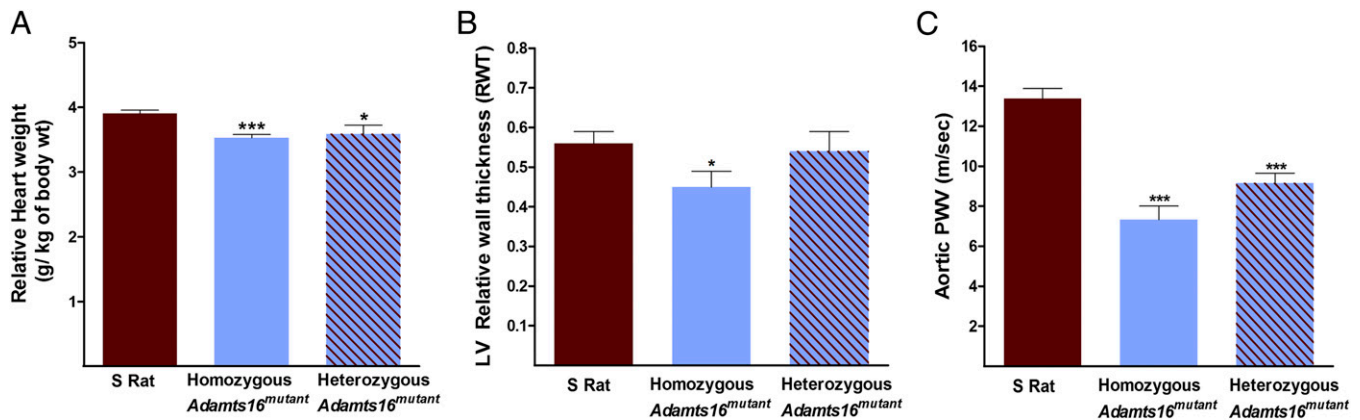


Fig. 3. Cardiac parameters of homozygous *Adamts16*^{mutant} ($n = 6$), heterozygous *Adamts16*^{mutant} ($n = 5$), and S ($n = 7$) rats. (A) Relative heart weight. (B) Left ventricular relative wall thickness. (C) Aortic pulse wave velocity. Left Ventricular (LV) RWT and aortic PWV were determined by echocardiography. Levels of statistical significance for all data were analyzed by ANOVA followed by Tukey's test; $*P < 0.05$, $***P < 0.001$.

microtubule-based, antenna-like organelles projecting from the apical surface of endothelial cells that are directly associated with collagen in the extracellular matrix (ECM). Immunohistochemical observation was suggestive of longer cilia within the endothelial cells of *Adamts16*^{mutant} rats compared with the S rats (Fig. 4B). This initial observation was further confirmed by scanning electron microscopic images of cilia (Fig. 4B). Cilia from the *Adamts16*^{mutant} rats were prominently elongated in the *Adamts16*^{mutant} rats compared with the cilia in the S rats (Fig. 4C).

Targeted Mutation in *Adamts16* Increased Proteinuria of the S Rats. Urinalysis was conducted to assess renal function of the *Adamts16*^{mutant} rats. Total protein content of the 24 h urine collected from *Adamts16*^{mutant} rats was significantly higher than that of the S rats (Fig. 5A), reminiscent of increased damage to kidney function in the *Adamts16*^{mutant} rats.

***Adamts16*^{mutant} Rats Exhibit Splitting and Thickened Glomeruli Capillaries.** To evaluate the histology of the kidneys, sections from S and *Adamts16*^{mutant} rats were examined (Fig. 5B). Jones silver staining showed thickened arteries in S rats, with extremely small lumen, whereas both homozygous and heterozygous *Adamts16*^{mutant} rats did not show thickening of the arteries (Fig. 5B and C). Further, splitting of the glomeruli capillaries was

observed in *Adamts16*^{mutant} rats (Fig. 5B). These results also point to vascular alterations within the kidneys of *Adamts16*^{mutant} rats.

***Adamts16*^{mutant} Rats Survive Longer than the S Rats.** Decreased BP and increased proteinuria were contrasting features of pathology of the *Adamts16*^{mutant} rats. To assess the outcome of these two dichotomously opposing phenotypes, the end points of survival of the rats were compared. The mean survival of the *Adamts16*^{mutant} rats was significantly ($P < 0.05$) longer than that of the S rats (Fig. 6).

Discussion

Adamts16 is one of 19 members of the ADAMTS family of metalloproteinases (14). Known functions of the ADAMTS proteases include processing of procollagens and von Willebrand factor as well as cleavage of aggrecan, versican, brevican, and neurocan (14, 15). They have been demonstrated to have important roles in connective tissue organization, coagulation, inflammation, arthritis, angiogenesis, and cell migration (14). Previously, our positional cloning strategy in rats pointed to *Adamts16* as one of only two positional candidate genes for BP within a highly resolved 804.6 kb region of the rat genome and demonstrated that variants of *Adamts16* are associated with human essential hypertension (8). The results of the present study, using a targeted mutant of

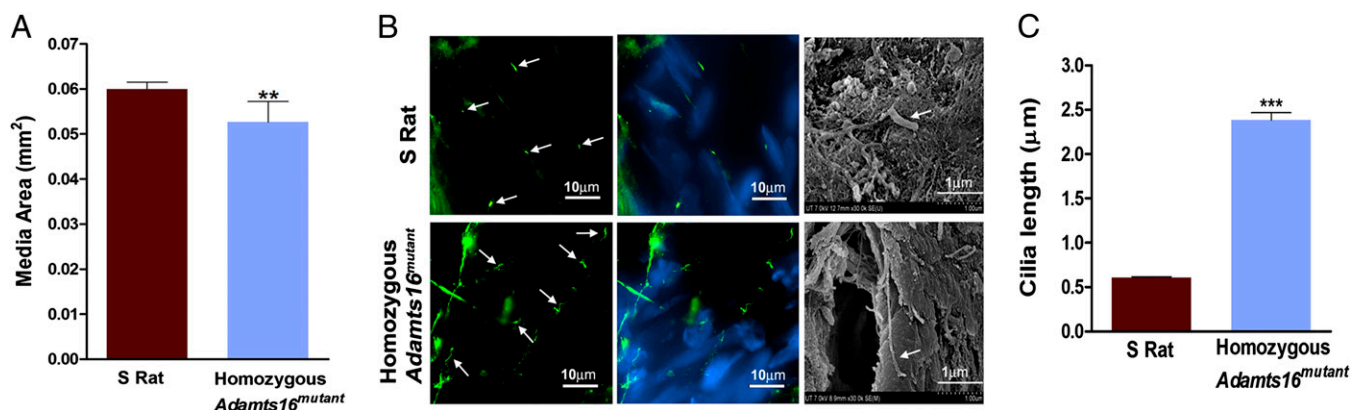


Fig. 4. Vascular features of homozygous *Adamts16*^{mutant} ($n = 6$) and S ($n = 7$) rats. (A) Quantitation of media area. (B) Images of vascular endothelial primary cilia. From left first and second panels, representative images of primary cilia from vascular endothelia observed by immunofluorescence microscopy. Arrows indicate green fluorescently labeled cilia. Cilia were stained with monoclonal acetylated α -tubulin (green), whereas the nuclei were stained with DAPI (blue). From left third panel, scanning electron micrographs of cilia in vascular endothelia; arrows point to cilia. (C) Quantitation of cilia length from scanning electron micrograph images. More than 200 cilia were counted in each strain; $**P < 0.01$, $***P < 0.001$.

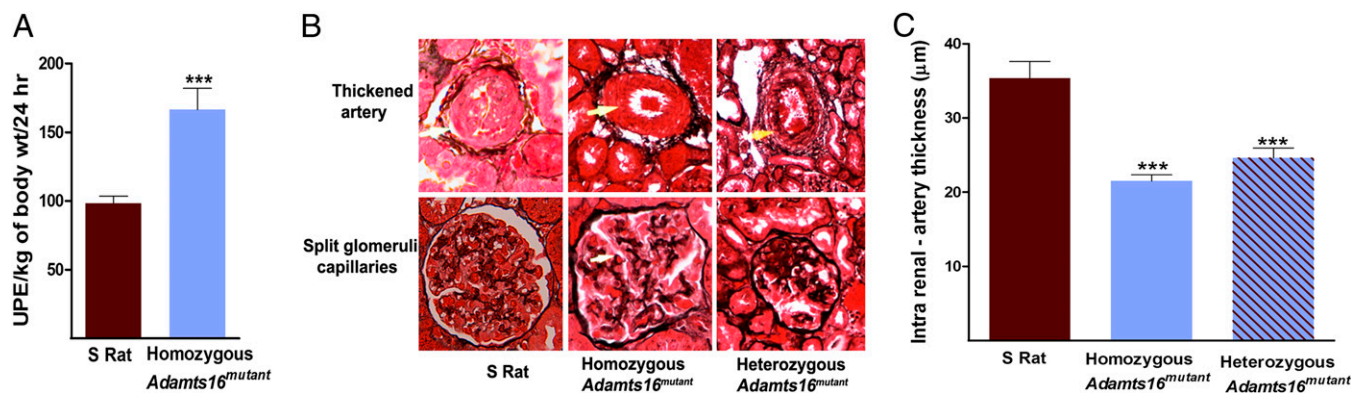


Fig. 5. Renal parameters of experimental groups of animals. (A) Total 24 h urine protein was assessed in S ($n = 15$) and homozygous *Adamts16*^{mutant} rats ($n = 12$) as described in the *Materials and Methods* section. (B) Representative Jones silver-stained kidney sections. Yellow arrows in the top panel point to thickened arteries. White arrow in the bottom panel center image from the kidney of a homozygous *Adamts16*^{mutant} rat shows split glomerular capillary. (C) Quantitation of intrarenal artery thickness shown in the top panel of B; $n = 3$ /group; *** $P < 0.0001$.

Adamts16, provide strong evidence to suggest that the function of this gene is linked to BP regulation. Further, the observation of lowering of hypertension in *Adamts16*^{mutant} rats coupled with large structural alterations in vessel architecture point to structural integrity of the vasculature as being tightly linked to the function of *Adamts16* in BP regulation.

Using the same gene targeting strategy described in our study, recently, one of the subunits of reduced nicotinamide adenine dinucleotide phosphate (*Nadph*) oxidase, *p*^{67Phox}, was reported to play an important role in salt-sensitive hypertension (16). Unlike the known function of the gene product of *p*^{67Phox} in scavenging reactive oxygen species (16), the function of *Adamts16* is not known. Therefore, to bridge the gap in knowledge between *Adamts16* and BP regulation, it will now be important to identify whether *Adamts16* is indeed a metalloproteinase, and if so, it will also be important to identify specific substrate/s and interacting partners of *Adamts16* in the vasculature.

The S rat model of hypertension is also a model of renal disease, which is primarily characterized by proteinuria. Increased pro-

teinuria observed in the *Adamts16*^{mutant} rats compared with S rats suggests that the function of *Adamts16* may not be limited to the vasculature. Future renal studies will be required to determine the extent to which *Adamts16* might be affecting BP by way of effects on glomerular filtration rate, renal hemodynamics, and renal handling of sodium.

The ZFN-based targeted gene editing strategy for *Adamts16* constitutes an important advancement and addition to the traditional congenic mapping of *Adamts16* as a gene regulating BP. However, because the ZFN-based gene editing strategy and the natural recombination-based congenic strategy are not directly comparable at the level of genome composition, to further reconcile our findings in this study with previous data obtained from S and S.LEW congenic rats (8), it will be necessary to combine the targeted disruption of the S genome at the *Adamts16* locus with a targeted insertion of the LEW rat allele of *Adamts16*.

Materials and Methods

Animals. All animal research protocols were preapproved by the University of Toledo's Institutional Animal Care and Use Committee and conducted as per the Guide for the Care and Use of Animals of the National Research Council. The Dahl Salt-sensitive (S) rats were from the colony inbred at the University of Toledo.

Generation of a ZFN-Mediated *Adamts16*^{mutant} Rat. ZFN construct pairs specific for the rat *Adamts16* gene were designed, assembled, and validated by Sigma-Aldrich to target the first exon of *Adamts16* (target sequence **CCGCGGTTGCTTTCGCTCTGGGTGCTGTTGCTGGCGCA**; ZFN binds to each sequence shown in bold on opposite strands). mRNA encoding the *Adamts16* ZFN pairs were diluted in RNase-free tris-EDTA buffer, pH 7.4 at a concentration of 2 ng/µL and injected into fertilized Dahl S rat eggs as described previously (17). Twenty rat egg donors produced 432 eggs, 137 were fertilized and microinjected, 116 eggs survived injection, and 106 eggs were transferred to pseudopregnant Sprague-Dawley females (Charles River Laboratory SAS SD rats), which gave birth to 37 rat pups. DNA was extracted (Wizard SV 96 Genomic DNA purification system, Promega) from tail tissue and was amplified using *Adamts16* ZFN Forward (5'ctgcagtgataactccgatg 3') and *Adamts16* ZFN Reverse (5'aggacacctagtaaaacgg 3') primers. PCR products were analyzed through 2% (wt/vol) agarose gel followed by DNA sequencing using MWG operon sequencing service. The sequencing data were analyzed using Sequencher 4.10.1. Among the 37 pups born, three positive heterozygous founder males were identified. The founder male rats were backcrossed to the same littermate of nonfounder females. Multiple separate pairs of mutation-carrying progeny were then intercrossed to generate an F2 population that was used for phenotyping and breeding to homozygosity. The DNA sequencing of the homozygous *Adamts16*^{mutant} rats showed a 17 bp deletion of the sequence "gctctgggtgctgttgc" in exon 1 of the *Adamts16* gene. Renal mRNA from all of the *Adamts16*^{mutant} homozygous animals reported in this study was extracted using TRIzol Reagent (Life Technologies), and cDNA was obtained by reverse transcription with SuperScript III

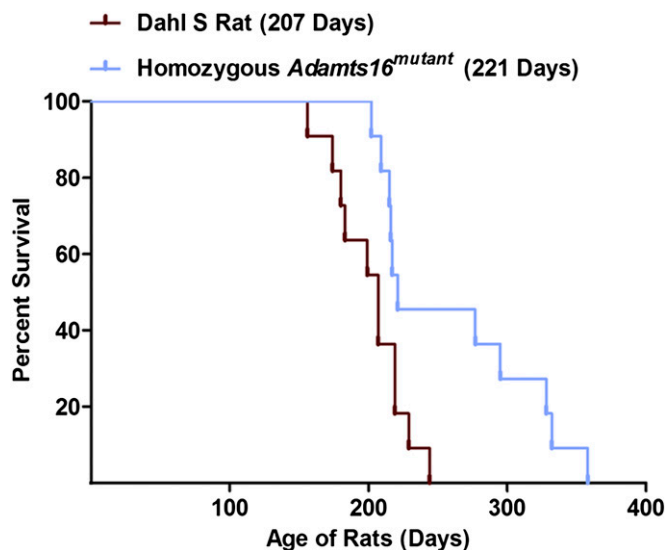


Fig. 6. Kaplan-Meier plot. Data from rats ($n = 10$ S rats and $n = 10$ *Adamts16*^{mutant} rats) in the survival study were plotted, and median survival of each group was calculated using the Graphpad prism software. Median survival of the *Adamts16*^{mutant} rats was greater than the survival of the S rats; * $P < 0.05$.

(Invitrogen) using an Oligo dT primer. The cDNA was PCR amplified using *Adamts16* exon-specific primers (sense 5' TAGCGGCCGCCACCATGGAAACCCGCGGTTGCTTTG 3' and antisense 5' CCAAGGTGAAAGTTGTCATGGTGCAG 3'). The PCR products were sequenced and all of the homozygous *Adamts16*^{mutant} rats were confirmed to harbor the 17 base pair deletion and stop codon in the first exon of the *Adamts16* transcript. Protein status of *Adamts16* could not be assessed, as specific antibodies to *Adamts16* were not available.

BP Measurements by Tail-Cuff and Radiotelemetry. Each set of homozygous *Adamts16*^{mutant} ($n = 6$ males), heterozygous *Adamts16*^{mutant} ($n = 5$ males), and parental strain 5 rats ($n = 7$ males) were bred, housed, and studied concomitantly to minimize environmental effects. Age-matched rats were weaned at 30 d of age and given a low-salt diet (0.3% NaCl, Harlan Teklad). Systolic BP measurements were obtained on all rats at 14.5 wk of age by the tail-cuff method as described previously (8). The week after the tail-cuff BP measurements, radiotelemetry experiments and statistical analyses were conducted as previously reported (8). Rats were euthanized after obtaining BP measurements, and total body weights and organ weights were collected.

Echocardiography. Left ventricular RWT of *Adamts16*^{mutant} ($n = 6$ males) and control 5 ($n = 7$ males) rat hearts was evaluated by echocardiography as described previously (18). To estimate aortic PWV, ECG and Doppler signals obtained from the carotid and the iliac arteries were recorded, and the path length (Lci, distance between the points of probe application on the carotid and iliac arteries) was measured using a tape measure. The time intervals between the R-wave of the ECG to the foot of the Doppler carotid and iliac waveforms were averaged over three cardiac cycles, and the pulse-transit time from the carotid-iliac (PTTci) was calculated by subtracting the mean R-carotid time interval from the mean R-iliac time interval. PWV of the abdominal aorta was then estimated using the following formula: $PWV = Lci/PTTci$.

Vascular Imaging. Vessels were fixed in 10% neutral buffered formalin followed by paraffin processing, embedding, and sectioning as previously described (19). Sections were de-paraffinized, stained with DRAQ5 (Biosstatus Limited) and imaged.

Confocal Microscopy of the ECM. A Leica TCS SP5 laser scanning confocal microscope (Leica Microsystems) equipped with a ti-sapphire tunable multiphoton laser (Coherent) was used to image collagen and elastin of the vessel wall. Collagen is a very bright second harmonic generator (hyperpolarizability) due to the shell of the collagen fibril (intrinsic tissue structure) and can be imaged either ex vivo or in vivo (20, 21). Second harmonic generation (SHG) for collagen was optimally imaged using 860 nm excitation multiphoton [(MP) laser] for maximum efficiency and emission collection was in the range of 425–435 nm with a peak emission generated at 430 nm (20, 21). Elastin also exhibits an inherent auto fluorescence and was excited at a wavelength of 488 nm with an emission in the range of 500–575 nm. Concurrently, nuclei within the vessels were stained with DRAQ5 and imaged at 647/681 nm. Images were acquired in 1 μ m z-stacks in a sequential manner at 10 \times and 20 \times magnification. Media area was calculated using Image J software by measuring the area between the internal and external lamina borders in 5 micron cross sections of the abdominal aorta.

Cilia Measurement and Analysis. Primary cilia were observed both with immunofluorescence and scanning electron microscopy as described previously (22).

Renal Histology. Kidneys from groups of rats ($n = 3$ /strain) were fixed in 10% neutral buffered formalin. Glomeruli capillary thickness and splitting were determined using Jones silver-stained sections (23). Three sections per animal ($n = 3$ /group) were used to determine the thickness of the glomeruli capillaries using Image Pro Plus, version 6.0.0.260.

Urinary Protein Excretion. Urinary protein excretion (UPE) determination was done as previously described (24).

Survival Study. *Adamts16*^{mutant} ($n = 10$ males) and 5 rats ($n = 10$ males) were weaned at 30 d of age and given a low-salt diet (0.3% NaCl, Harlan Teklad). The rats were switched to a high-salt-containing diet (2% NaCl, Harlan Teklad) on day 124 and continued on the 2% NaCl diet until their natural death.

ACKNOWLEDGMENTS. This work was funded by National Institutes of Health Grants HL076709, HL020176, and HL112641 (to B.J.) and an American Heart Association fellowship (Great Rivers Affiliate, 09POST2400144 to E.E.M.).

1. Simino J, Rao DC, Freedman BI (2012) Novel findings and future directions on the genetics of hypertension. *Curr Opin Nephrol Hypertens* 21(5):500–507.
2. Cowley AW, Jr., et al. (2012) Report of the National Heart, Lung, and Blood Institute Working Group on epigenetics and hypertension. *Hypertension* 59(5):899–905.
3. Cowley AW, Jr. (2006) The genetic dissection of essential hypertension. *Nat Rev Genet* 7(11):829–840.
4. Joe B, Garrett MR (2006) *Genetic Analysis of Inherited Hypertension in the Rat. Genetics of Hypertension, Handbook of Hypertension*, eds Dominiczak A, Connell J (Elsevier Science, Amsterdam), Vol 24, pp 177–200.
5. Rice T, et al. (2000) Genome-wide linkage analysis of systolic and diastolic blood pressure: The Québec Family Study. *Circulation* 102(16):1956–1963.
6. Joe B, Garrett MR, Dene H, Rapp JP (2003) Substitution mapping of a blood pressure quantitative trait locus to a 2.73 Mb region on rat chromosome 1. *J Hypertens* 21(11):2077–2084.
7. Garrett MR, et al. (1998) Genome scan and congenic strains for blood pressure QTL using Dahl salt-sensitive rats. *Genome Res* 8(7):711–723.
8. Joe B, et al. (2009) Positional identification of variants of *Adamts16* linked to inherited hypertension. *Hum Mol Genet* 18(15):2825–2838.
9. Saad Y, Garrett MR, Lee SJ, Dene H, Rapp JP (1999) Localization of a blood pressure QTL on rat chromosome 1 using Dahl rat congenic strains. *Physiol Genomics* 1(3):119–125.
10. Saad Y, Garrett MR, Rapp JP (2001) Multiple blood pressure QTL on rat chromosome 1 defined by Dahl rat congenic strains. *Physiol Genomics* 4(3):201–214.
11. Geurts AM, et al. (2009) Knockout rats via embryo microinjection of zinc-finger nucleases. *Science* 325(5939):433.
12. Lehmann ED (1999) Clinical value of aortic pulse-wave velocity measurement. *Lancet* 354(9178):528–529.
13. Laurent S, et al. (2001) Aortic stiffness is an independent predictor of all-cause and cardiovascular mortality in hypertensive patients. *Hypertension* 37(5):1236–1241.
14. Stanton H, Melrose J, Little CB, Fosang AJ (2011) Proteoglycan degradation by the ADAMTS family of proteinases. *Biochim Biophys Acta* 1812(12):1616–1629.
15. Gao W, et al. (2012) Rearranging exosites in noncatalytic domains can redirect the substrate specificity of ADAMTS proteases. *J Biol Chem* 287(32):26944–26952.
16. Feng D, et al. (2012) Increased expression of NAD(P)H oxidase subunit p67(phox) in the renal medulla contributes to excess oxidative stress and salt-sensitive hypertension. *Cell Metab* 15(2):201–208.
17. Filipiak WE, Saunders TL (2006) Advances in transgenic rat production. *Transgenic Res* 15(6):673–686.
18. Gopalakrishnan K, et al. (2011) Augmented rifylin is a risk factor linked to aberrant cardiomyocyte function, short QT interval and hypertension. *Hypertension* 57(4):764–771.
19. Nestor AL, et al. (2006) Linkage analysis of neointimal hyperplasia and vascular wall transformation after balloon angioplasty. *Physiol Genomics* 25(2):286–293.
20. Williams RM, Zipfel WR, Webb WW (2005) Interpreting second-harmonic generation images of collagen 1 fibrils. *Biophysical Journal* 88:1377–1386.
21. Zoumi A, Lu X, Kassab GS, Tromberg BJ (2004) Imaging coronary artery microstructure using second-harmonic and two-photon fluorescence microscopy. *Biophysical Journal* 87:2778–2786.
22. Abdul-Majeed S, Nauli SM (2011) Dopamine receptor type 5 in the primary cilia has dual chemo- and mechano-sensory roles. *Hypertension* 58(2):325–331.
23. Jones DB (1957) Nephrotic glomerulonephritis. *Am J Pathol* 33(2):313–329.
24. Kumarasamy S, et al. (2011) Refined mapping of blood pressure quantitative trait loci using congenic strains developed from two genetically hypertensive rat models. *Hypertens Res* 34(12):1263–1270.